JOURNAL OF MATERIALS SCIENCE 24 (1989) 124–132

On the orthorhombic phase in ZrO_2-based alloys

A. H. HEUER, V. LANTERI*, S. C. FARMER‡, R. CHAIM§, R.-R. LEE¶, B. W. KIBBEL**, R. M. DICKERSON
Department of Materials Science and Engineering, Case Western Reserve University, Cleveland, Ohio 44106, USA

During TEM observation, a tetragonal (t) to orthorhombic (o) phase transformation often occurs in thin portions of ZrO_2-containing foils. This transformation is stress-induced and in some senses artefactual, in that the reaction product is actually a high-pressure phase, relative to monoclinic (m) ZrO_2, that can form from metastable t-ZrO_2 in the TEM because its density is intermediate between t- and m-ZrO_2. Examples of the formation of o-ZrO_2 in a number of different systems are given.

1. Introduction

The polymorphism of pure ZrO_2 at atmospheric pressure has been extensively studied [1–7]. The high-temperature polymorph has cubic (c) symmetry and has the fluorite structure; the intermediate temperature tetragonal (t) form and the low-temperature monoclinic (m) form are both distorted versions of the fluorite structure. Alloying with various stabilizing solutes such as MgO, CaO, Y_2O_3, or CeO_2 affects the polymorph stability and, depending on heat treatment and composition, can result in multiphase materials (c + t, c + t + m, c + m, or t + m) at room temperature (partially stabilized zirconia, PSZ), or fully cubic material (fully stabilized zirconia, FSZ). Several authors [8–13] have also found a non-equilibrium tetragonal phase (t′-ZrO_2) in Y_2O_3–ZrO_2 alloys with high Y_2O_3 contents, that forms diffusionlessly from c-ZrO_2 during rapid cooling from high temperatures.

The polymorphism of pure ZrO_2 and its alloys was recognized many years ago and forms the basis for the well-known phenomenon of transformation toughening [14, 15]. In recent years, however, additional polymorphs in ZrO_2-based alloys have been reported. Hasegawa and co-workers have reported that a rhombohedral phase (r-ZrO_2) forms either on abraded surfaces [16] or in ion-implanted layers [17] of Y-PSZ. Early work by Bendeliani *et al.* [18] showed evidence of a high-pressure (4 to 11 GPa) phase with orthorhombic (o) symmetry, which was confirmed later by Bocquillon and Susse [19]. Liu [20] reported yet a different orthorhombic phase with the cotunnite ($PbCl_2$) structure after quenching from pressures above 10 GPa and temperatures of 100° C. Block, *et al.* [21] found a "pseudo-tetragonal" polymorph at pressures above 4.4 GPa (at room temperature), with subsequent transformation to the cotunnite orthorhombic phase at pressure above 16.5 GPa. Finally Suyama, *et al.* [22] synthesized powders of o-ZrO_2 and of o-$Hf_{1-x}Zr_xO_2$ by quenching from high temperature and high pressure; Kudoh *et al.* [23] performed a high-pressure structural analysis of this phase.

There have also been reports [24–34] of o-ZrO_2 in transmission electron microscope (TEM) thin foils, although X-ray diffraction (XRD) experiments, performed on similar bulk materials, showed no evidence of this phase. Heuer and co-workers observed a t → o transformation in Mg-PSZ alloys, either on fracture surfaces [24] or in thermally-shocked [25–28] materials; the formation of o-ZrO_2 in Mg-PSZ has been confirmed by other workers [29, 30]. Orthorhombic symmetry was also found in ZrO_2 precipitates formed in Cu–Zr alloys by internal oxidation. [31]. o-ZrO_2 has also been reported in Ca-PSZ, [32] in Y_2O_3–ZrO_2 alloys [33, 34] and in a ternary (Mg, Y)-TZP (tetragonal ZrO_2 polycrystal) [35].

With the exception of the very high-pressure cotunnite phase, all these reports of o-ZrO_2 are believed to refer to a distorted fluorite structure, whose structure has been reported by Kudoh *et al.* [23]. This phase has a well-defined thermodynamic stability region, as shown on the *T–P* phase diagram of pure ZrO_2 in Fig. 1, but will form from metastable t-ZrO_2 in various ZrO_2 alloys.

The aim of this paper is to report new TEM thin-foil observations of o-ZrO_2 in various ZrO_2-based alloys: Mg-PSZ, Y-PSZ, Ca-PSZ, ternary (Mg, Ca)- and (Mg, Y)-PSZ and ZrO_2-toughened Al_2O_3 (ZTA). Based on these observations, we suggest that the formation of the orthorhombic phase from metastable t-ZrO_2 particles in TEM thin foils is always artefactual; however, we note that Marshall *et al.* and James [36] have found o-ZrO_2 in bulk samples of supertough Mg-PSZ cooled below room temperature.

2. Experimental procedure and results

We have found that o-ZrO_2 forms from t-ZrO_2 in every ZrO_2-containing ceramic we have studied, regardless of composition and heat-treatment, although the propensity to undergo this transformation does vary. TEM specimens were prepared following the standard methods of sectioning and mechanical thinning to a

Current affiliations: *IRSID, St. Germain en Laye, France; ‡NASA Lewis Research Center, Cleveland, Ohio; §Technion, Haifa, Israel; ¶CPS, Inc., Cambridge, Massachusetts; **General Motors Research Laboratory, Detroit, Michigan.

0022–2461/89 $03.00 + .12

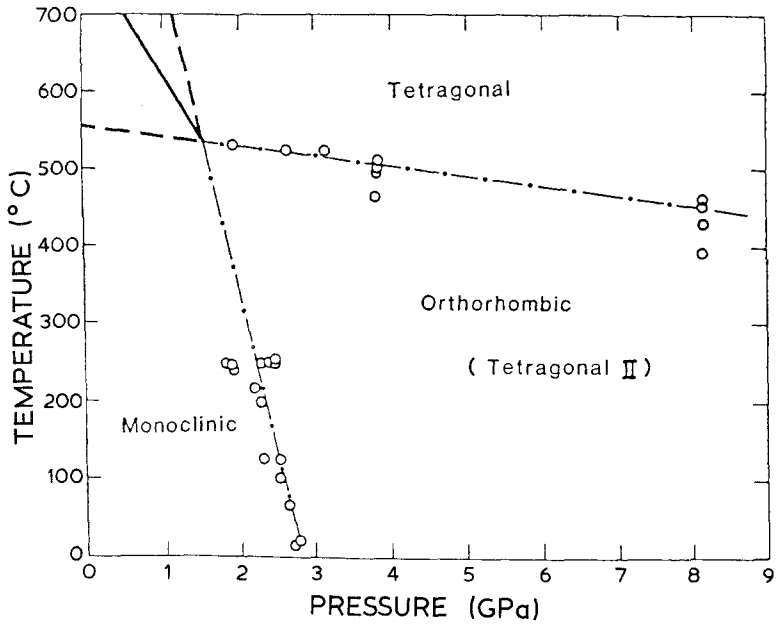

Figure 1 P–T phase diagram of pure ZrO_2 (the heavy dashed lines are metastable extensions of the dash-dot solvuses). Diagram taken from H. Arashi [37].

thickness of about 60 μm, followed by "dimpling" and ion-thinning with 6 kV Ar^+ ion until perforation. The specimens were coated with a thin carbon layer to avoid charging during observation in a Philips 400T EM operating at 120 kV.

2.1. Mg-PSZ

This system has been the most extensively studied by TEM and shows many features that will be used to interpret the t → o transformation in all ZrO_2-based systems. The heat-treatments used to form strong and tough Mg-PSZ containing t-ZrO_2 precipitates are now well known, [14, 15]. o-ZrO_2 is thus present as discrete particles in Mg-PSZ, having transformed from t-ZrO_2 precipitates; the lattice parameters are quite different from the high temperature–high pressure orthorhombic phase reported by Liu [20]. This orthorhombic phase was first observed in TEM foils of thermally shocked materials [25–28] although two orthorhombic forms were actually identified [27] and referred to as o- and o′-ZrO_2; the lattice parameters of the former [28] are $a_o = 0.508$ nm, $b_o = 0.518$ nm, $c_o = 0.508$ nm (Table I), while the lattice parameters for o′-ZrO_2 are $a_{o'} \cong 2a_o$, $b_{o'} \cong b_o$ and $c_{o'} \cong c_o$; the space groups of these phases were determined (from high-angle tilting experiments and analysis of selected-area diffraction (SAD) patterns) to be Pbcm and Pbca, respectively [27]. In many samples of Mg-PSZ, heat-treated to increase the transformability of t-ZrO_2, the precipitates transform to orthorhombic symmetry in the thinner regions of the foil during routine TEM examination. In thicker regions of these same foils, the t → o transformation does not occur. The t → o transformation also occurs adjacent to cracks which form accidently during foil preparation, as shown in Fig. 2a. It is interesting to note that in this example, the t-ZrO_2 precipitates transformed to monoclinic symmetry in the most highly-stressed region immediately adjacent to the crack surface, while those precipitates located farther from the crack surface transformed to orthorhombic symmetry. Lenz and Heuer [24] speculated that the t → m transformation in bulk materials might always by two-step –t → o → m– as in this example, but no evidence exists to support this notion for the bulk martensitic transformation.

Some particles of o-ZrO_2 in Mg-PSZ show heavy faulting, while others show uniform contrast. Using a convention consistent with the Pbcm determination of reference [23] and the data of Table I, the faulting is found to occur primarily along the $(0\,1\,0)_o$ trace. Half-order maxima are observed for a number of orientations in SAD patterns (Fig. 2b). A dark-field image formed using the half-order maxima (corresponding to an approximately 1.0 nm interplanar spacing) is shown in Fig. 2c. Subsidiary maxima along a streak can be due to a high density of regularly spaced faults (the fault spacings in Fig. 2c range from 2.5 to 4.0 nm), and it becomes a semantic issue whether or not to call such a faulted crystal a new phase (the o′-ZrO_2 with apparent Pbca symmetry [27]). o-ZrO_2 in Mg-PSZ has also been studied by high-resolution electron microscopy (HREM) [30]; the Pbcm space group was confirmed for the orthorhombic product by comparing HREM images with computer-simulated images based on the structure reported by Kudoh *et al.* [23].

Finally, a rare example (for Mg-PSZ) of linear defects having the contrast of anti-phase domain boundaries (APBs) is shown by the "in-plane" precipitates in Fig. 2d; diffraction analysis reveals that these particles now have monoclinic symmetry. As is discussed in detail in the next section, such APBs often occur during the t → o transformation in Y-PSZ and can be inherited in m-ZrO_2 if a subsequent thin-foil

TABLE I Lattice parameters of o-ZrO_2 determined by TEM

System	t-ZrO_2		o-ZrO_2			$\Delta V_{t\to o}$
	a_t(nm)	c_t(nm)	a_o(nm)	b_o(nm)	c_o(nm)	
Mg-PSZ	0.507(7)	0.518(3)	0.508	0.52(3)	0.51(7)	+0.1%
Y-PSZ	0.511(6)	0.515(7)	0.509	0.52(9)	0.51(7)	+3.1%
Ca-PSZ	0.509(4)	0.518(0)	0.509	0.52(4)	0.51(2)	+1.7%
ZTA*	0.508(2)	0.518(9)	0.5005	0.5235	0.5051	+1.3%

*The lattice parameters are for pure ZrO_2 and are included for convenience. a_t and c_t were taken from Lanteri *et al.* [37] while a_o, b_o and c_o are from Kudoh *et al.* [23].

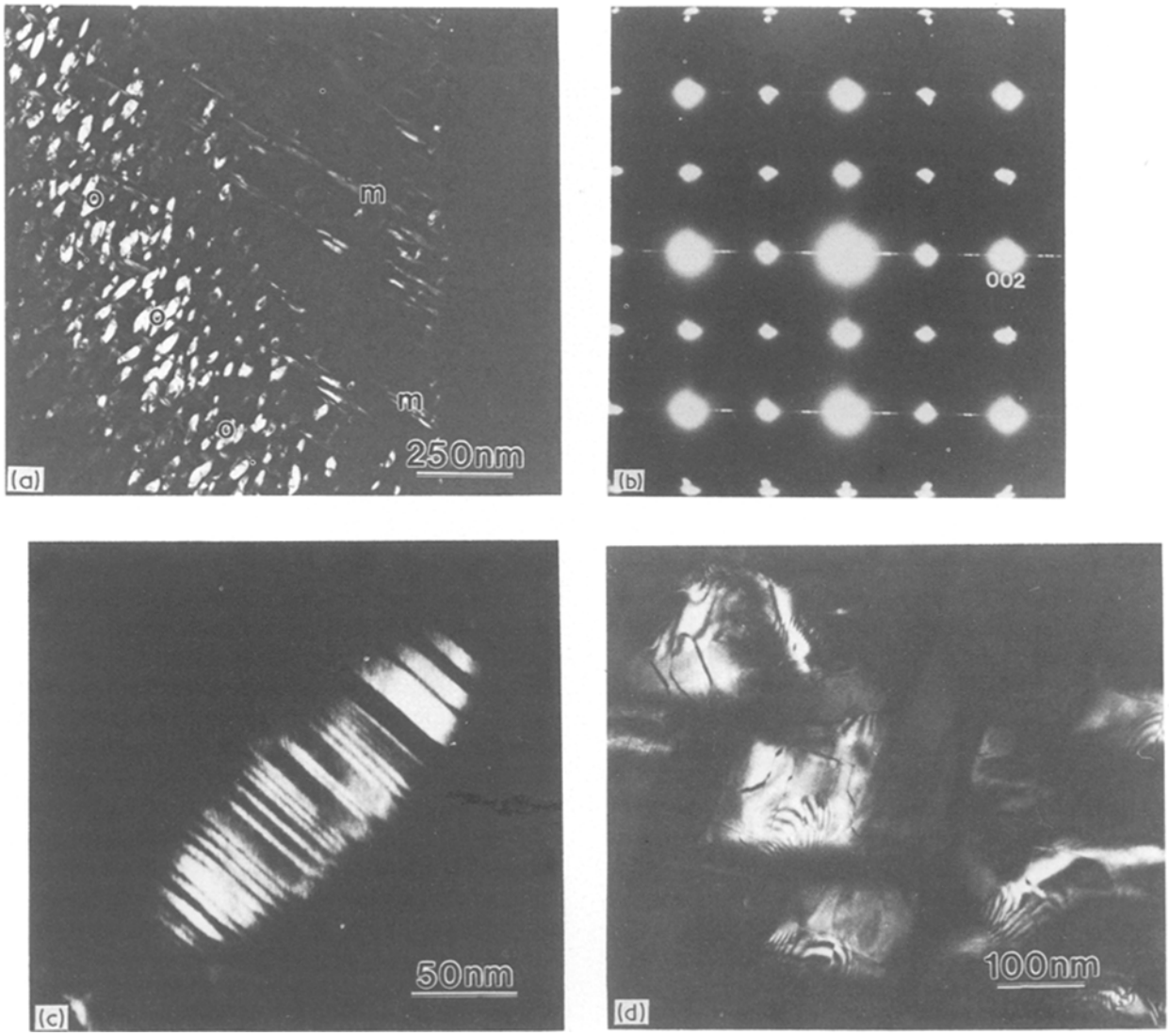

Figure 2 (a) Dark-field micrograph of Mg-PSZ showing monoclinic precipitates (m) near the crack (the dark vertical feature on the right) and orthorhombic precipitates (o) farther away. (b) SAD pattern ([1 0 0] zone axis), from the region of (a) containing orthorhombic precipitates (c) Dark-field micrograph of an orthorhombic precipitate, showing heavy planar faulting on $(0\,1\,0)_o$ planes. (d) Dark-field micrograph of monoclinic orthorhombic (originally) precipitates showing curvilinear APB-like defects within particles.

o → m transformation occurs. We suggest a similar origin for the linear defects of Fig. 2d.

2.2. Y-PSZ

Skull-melted 8 wt % Y-PSZ single crystals were annealed at 1600° C for 50 h to develop the equilibrium two-phase (c + t) microstructure. The as-received material contained small t-ZrO_2 particles formed by homogeneous precipitation in a cubic matrix, which matrix undergoes the c → t′ displacive transformation during cooling [11]. Annealing at high temperatures results in the coarsening of the t-ZrO_2 precipitates into a "colony" structure, which consists of stacks of two twin-related t-ZrO_2 variants sharing the same habit plane, $(1\,0\,1)_t$ or $(0\,1\,1)_t$, but whose *c* axes are at nearly 90°. (The actual angle between the *c* axes of the two variants is about 89°, due to the small (~1%) tetragonality of t-ZrO_2.) The two variants fits nearly perfectly on the $\{1\,0\,1\}_t$ plane without appreciable lattice strain [39, 40], as has been verified using HREM [41].

Fig. 3a is a SAD pattern taken from the t-ZrO_2 colonies oriented to the ⟨1 0 0⟩ zone axis. The fine structure within the {0 2 2} reflections (the arrowed spots) is due to the two twin-related t-ZrO_2 variants within each colony. During TEM observation, some of the t-ZrO_2 colonies, especially those located in very thin areas (i.e. near the perforation in the TEM foil), transformed to orthorhombic symmetry. This transformation occurred so rapidly that it was not possible to follow the transformation sequence in detail. Several forward and reverse t → o phase transformations could be observed, however, the reverse (o → t) transformation being induced by using the electron beam as a heating source.

The transformed areas often contained APBs within individual twins (Figs. 3b and c). An SAD pattern in the ⟨1 0 0⟩ zone axis, from the transformed colonies containing APBs, shows $\{0\,0\,1\}_t$ and $\{0\,1\,0\}_t$ extra reflections (Fig. 3d) forbidden for t-ZrO_2 but characteristic of orthorhombic symmetry in this case. (Wide-angle tilting experiments were performed to confirm that m-ZrO_2 was not present to account for these otherwise-forbidden reflections.)

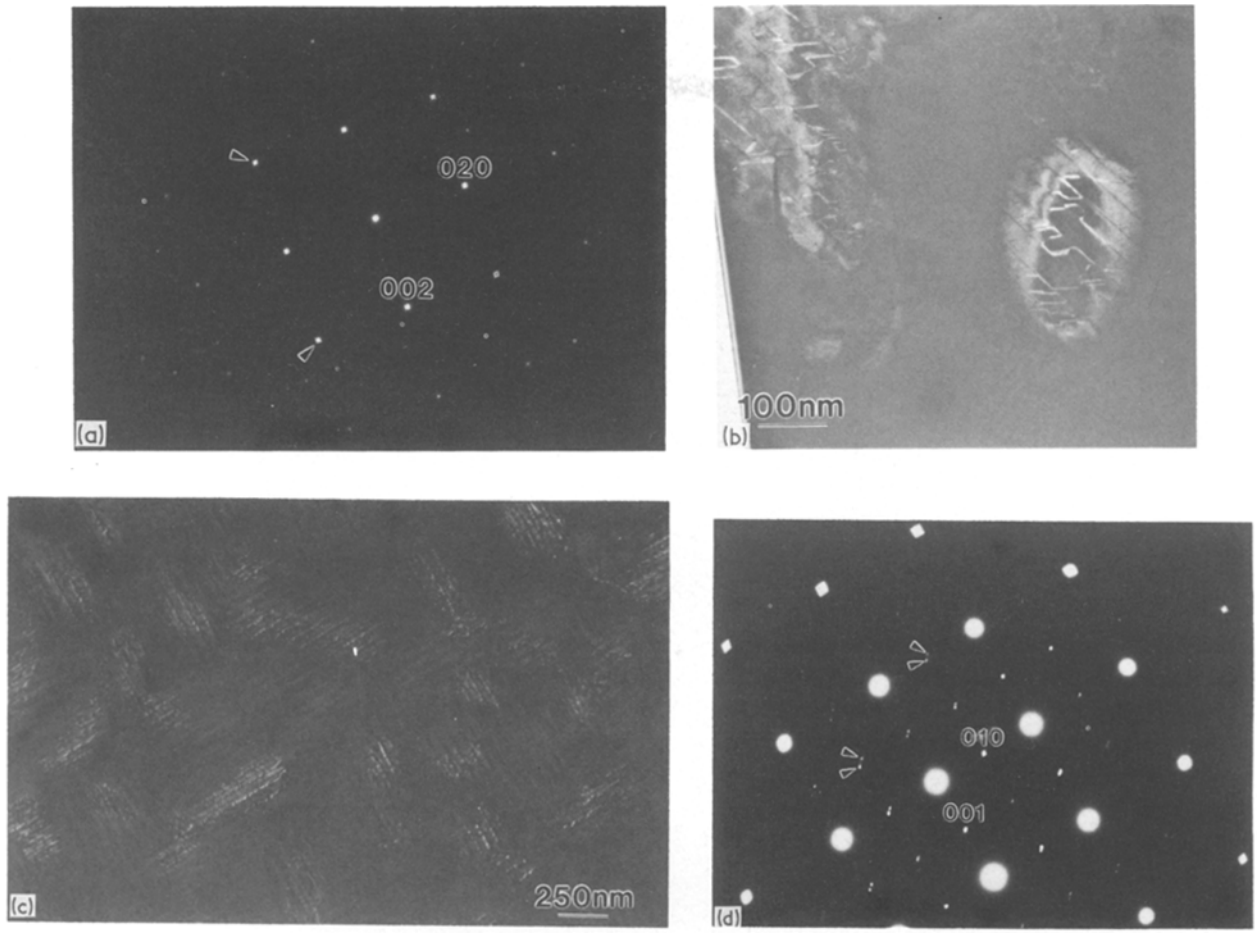

Figure 3 (a) SAD pattern ([1 0 0] zone axis) from t-ZrO_2 colonies in Y-PSZ. (b) Dark-field micrograph showing orthorhombic colonies with APBs. (c) Lower-magnification view of (b). (d) SAD pattern ([1 0 0] zone axis) from orthorhombic colonies.

The splitting of the extra spots (arrowed in Fig. 3d) clearly indicates that both t-ZrO_2 variants in the colony have transformed to orthorhombic symmetry. Streaks are also present in several different low-index SAD patterns. One possible origin for these streaks, as in the case of Mg-PSZ, is one-dimensional faulting in the o-ZrO_2 lattice, which originates during the t → o transformation (see section 4).

Diffraction analysis has shown that, with the crystallographic convention referred to above for orthorhombic crystals, the orientation relationship is $[0\,0\,1]_t \parallel [1\,0\,0]_o$ and $[1\,0\,0]_t \parallel [0\,0\,1]_o$. The lattice parameters of o-ZrO_2 in this alloy determined by TEM are included in Table I. As discussed in other work from our laboratory on the t → o transformation in individual t-ZrO_2 grains in a 4.5 mol % polycrystalline Y_2O_3–ZrO_2 alloy [34], which also show the same orientation relationship, the reduction in crystal symmetry accounts not only for the extra reflections observed in SAD patterns, but also for the formation of APBs via a mechanism similar to that postulated for the c → t′ transformation [11, 33]; the orthorhombic phase can nucleate at different lattice sites within a given tetragonal variant, and the impingement of such growing domains can result in APBs.

The stability of o-ZrO_2 within the colonies was studied by re-focusing the electron beam, which resulted in the sudden disappearance of the APBs. SAD patterns before and after the t → o transformation showed that the transformed orthorhombic colonies re-transformed to tetragonal symmetry, and the twin-related tetragonal variants were recovered. In some cases, however, the orthorhombic phase transformed martensitically to monoclinic symmetry, resulting in a microstructure of interpenetrating twins with the pre-existing, original $\{1\,0\,1\}_t$ twin planes still visible (Fig. 4). The presence of APBs within the transformed monoclinic colonies is an indication that in this instance, a two-step reaction had occurred (t → o → m) during the overall t → m reaction; the APBs are inherited by m-ZrO_2 from o-ZrO_2.

2.3. Ca-PSZ and (Mg, Ca)-PSZ

An artefactual t → o transformation in thin-foil specimens in 7.8 mol % Ca-PSZ has been described in the Appendix to Dickerson *et al.* [32]. However, only sparse details were given there, which will be elaborated on here.

Zone-axis diffraction patterns, most notably the $\langle 0\,0\,1 \rangle$ zone, often showed additional reflections forbidden for both the cubic and tetragonal polymorphs but without the twin-induced spot splitting associated with several variants of m-ZrO_2. In some cases, $\frac{1}{2}(1\,0\,0)_o$ streaks were present in the $\langle 0\,1\,2 \rangle$ and $\langle 0\,1\,1 \rangle$ zone-axis diffraction patterns, and were associated with fine, parallel striations, 1 to 3 nm in width, within the precipitates.

Analysis of a number of diffraction patterns in areas

Figure 4 Bright-field micrograph of monoclinic colonies showing APBs inherited from orthorhombic colonies (arrowed).

containing the orthorhombic phase showed the same orientation relationship as in Y-PSZ, and similar lattice parameters (Table I). Further analysis of a series of different zone-axis diffraction patterns, taken from the same area of a particular foil, showed that the three unit-cell axes were accurately perpendicular, conclusively demonstrating that the precipitates do not have rhombohedral or monoclinic symmetry.

The transformed precipitates occasionally showed fine striations in dark-field images (see Fig. A1 in Dickerson *et al.* [32]); curvilinear APBs such as those observed in Y-PSZ are also present, although they are much rarer (Fig. 5a). (The striated particles in the last figure have monoclinic symmetry.)

o-ZrO_2 particles in this system occasionally show linear alignment along $\langle 1\,0\,0 \rangle_c$ directions, usually in partially-transformed grains (see Fig. A2, in [32]), suggesting that the t → o transformation has an autocatalytic component. This alignment, which was previously reported [42] as an aspect of the precipitation of t-ZrO_2, could not be found in c-ZrO_2 grains in which all the precipitates had tetragonal symmetry.

Diffraction information from two o-ZrO_2 variants are seen in all of the $\langle 0\,0\,1 \rangle$ zone-axis diffraction

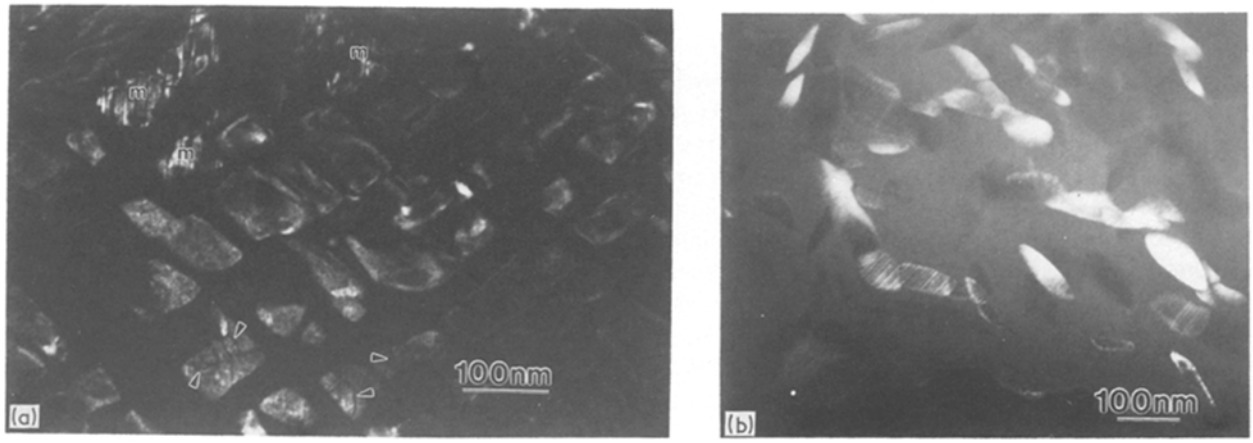

Figure 5 (a) Dark-field micrograph of orthorhombic precipitates in Ca-PSZ, showing APB-like defects (arrowed regions). Monoclinic precipitates (m) are also present in this region of the foil. (b) Dark-field micrograph of orthorhombic precipitates in (Mg, Ca)-PSZ.

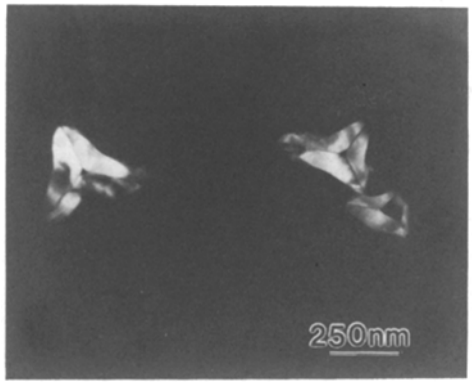

Figure 6 Dark-field micrograph of orthorhombic precipitates in (Mg, Y)-PSZ.

patterns in this system. These can, as previously noted, be identified by the presence of split reflections at positions forbidden for tetragonal and cubic symmetry, and by the distortions of the fundamental reflections. The two variants have their ***a*** (shortest lattice parameter) and ***b*** (longest lattice parameter) axes coplanar and rotated by 90° with respect to one another; the ***b*** axes are parallel and normal to the plane of the foil.

The fraction of orthorhombic particles decreases rapidly with distance from the foil edge. However, this fraction increases with repeated observation under the electron beam, and with time after foil preparation, clearly suggesting that the t → o transformation is induced by stresses arising from localized beam heating; the o → m transformation in this system can be induced by focusing the electron beam and thus creating much larger thermoelastic stresses.

The microstructure of a ternary (Mg, Ca)-PSZ, containing 4.5 mol % MgO and 4.5 mol % CaO, sintered at 1700° C for 4 h and slowly cooled and then reheated at 1400° C for 4 h, is shown in Fig. 5b. The t → o transformation has occurred in this region of foil, resulting in both striated and APB-containing particles.

2.4. (Mg, Y)-PSZ

The morphology of the tetragonal precipitates in a ternary (Mg, Y)-PSZ containing 2.62 mol % MgO and 4.45 mol % Y_2O_3 has been analyzed by TEM [43].

Fig. 3 of Lee and Heuer [43] shows dark-field images of three t-ZrO_2 variants formed using the three $\{1\,1\,2\}_t$ reflections near the $\langle 1\,1\,1\rangle$ zone axis; each precipitate is formed by the juxtaposition of three t-ZrO_2 variants. In some cases, however, generally near the edge of a foil in a $\langle 1\,1\,1\rangle$ orientation, the whole precipitate could be imaged with a single $\{1\,1\,2\}_t$ reflection, which could not occur if the composite particle was composed of three t-ZrO_2 variants (Fig. 6). Careful inspection of SAD patterns in $\langle 1\,0\,0\rangle$ and $\langle 1\,1\,1\rangle$ orientations revealed the orthorhombic symmetry of the precipitate; the precipitates of Fig. 6 are actually being imaged with three overlapping $\{1\,1\,2\}_o$ reflections.

2.5. ZrO_2-toughened Al_2O_3 (ZTA)

o-ZrO_2 has also been found in the dispersion-toughened ceramic, ZrO_2-toughened Al_2O_3 (ZTA). In this material the t-ZrO_2 exists as second-phase particles physically dispersed in a polycrystalline Al_2O_3 matrix. The ZrO_2 particles can be intergranular, i.e. located between Al_2O_3 grains, or because of matrix grain growth can become intergranular, i.e. trapped within Al_2O_3 grains.

The ZTA studied contained 12 vol % ZrO_2; its fabrication is described elsewhere [44]. Sintering in air for 2 h at 1450° C was followed by hot isostatic pressing for 10 min at 1600° C. The material was then heated for 32 h at 1550° C to cause Al_2O_3 grain and ZrO_2 particle growth.

Several intragranular particles in the same Al_2O_3 grain transformed during observation. Transformed particles with monoclinic symmetry (not shown here) were twinned, while other transformed particles contained irregular "domains" with non-distinct boundaries (Fig. 7a). Analysis (not shown here) of the SAD pattern revealed that $a_o \sim 2a_t$, thus indicating the presence of o′-ZrO_2.

HREM has been used to image another intragranular o′-ZrO_2 particle in this ZTA (Fig. 7b); the ~1 nm spacing is readily visible. Image simulations [45] of HREM images of such particles are particularly effective in establishing or confirming the crystal structure of the material of the micrograph. A particle subject to such analysis is shown in Fig. 8a; in this case no particular features characteristic of o-ZrO_2 are visible, although the SAD pattern (shown in

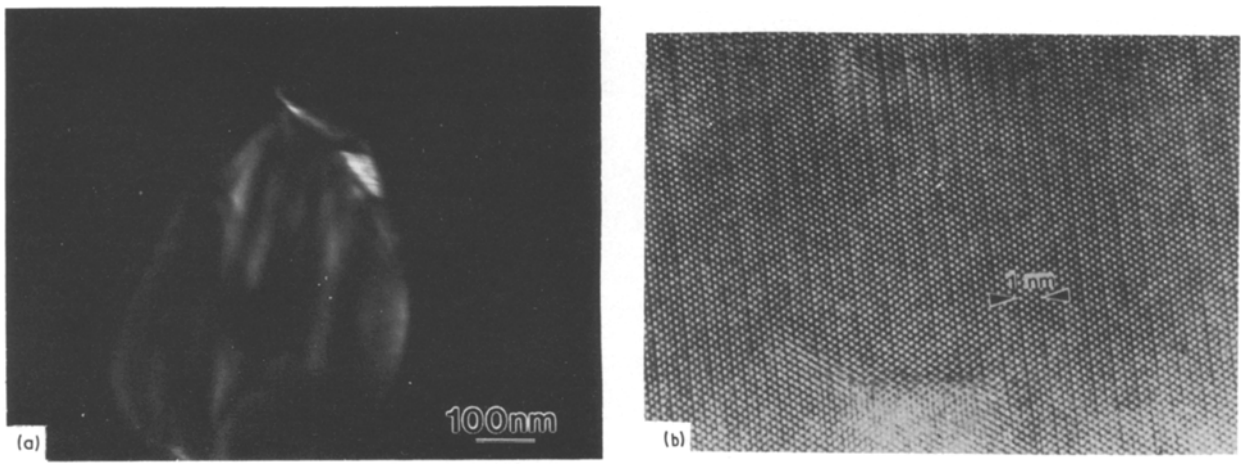

Figure 7 (a) Dark-field micrograph of o′ particle. (b) High-resolution electron micrograph of orthorhombic particle near Scherzer defocus.

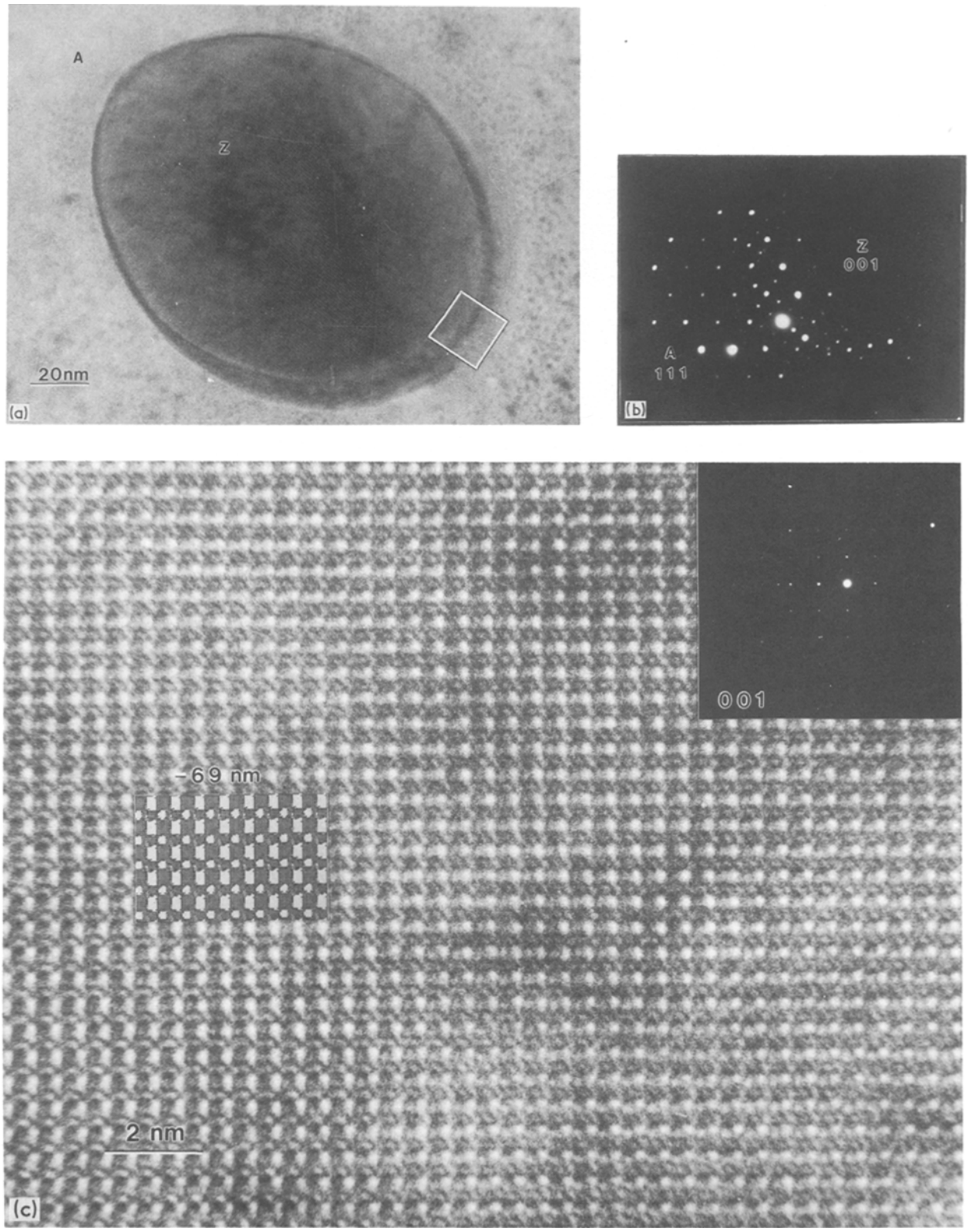

Figure 8 (a) Low-magnification image of o-ZrO_2 particle (Z) in an Al_2O_3 matrix (A). The outlined area is shown in (c) at high resolution. (b) Corresponding SAD pattern of both ZrO_2 ([0 0 1] zone axis) and Al_2O_3 ([1 1 1] zone axis). (c) HREM image of the outlined area in (a). The insets show the SAD pattern of the ZrO_2 particle, and an image match produced using the SHIRLI program [44]. The best image matching was found for a thickness of 15 nm and a defocus of −69 nm. The parameters used in the SHIRLI simulation are: lattice parameters $a_o = 0.5005$ nm, $b_o = 0.5235$ nm $c_o = 0.5051$, zone axis orientation [0 0 1], crystal tilt 2.222 mrad, beam tilt 0.243 mrad, objective aperture radius 7.3 nm, half-width of vibration 0.045 nm, half-width of spread of focus 6.0 nm, $C_s = 1.10$ nm, semi-angle of beam convergence 1.00 mrad. The lattice parameters of the orthorhombic phase were taken from Kudoh *et al.* [23].

Fig. 8b) clearly shows that the particle no longer has tetragonal symmetry but has transformed. Due to the small tilt capabilities of the high-resolution electron microscope it was not possible to carry out large-angle tilting experiments to distinguish between monoclinic and orthorhombic symmetry. Image simulations [45] were therefore performed on a series of through-focus micrographs to determine the symmetry of the particle. It was not possible to match the experimental images by assuming the particle had

monoclinic symmetry; however, assuming the orthorhombic structure (in reference [23]) it was possible to match the experimental and computed through-focus images for a number of defocus conditions. Such good matching is shown in one case near Scherzer defocus (Fig. 8c).

3. Group theoretical considerations

It is now clear that the t → o transformation in ZrO_2 can occur in several different instances. According to Kudoh *et al.* [23] the space group of the orthorhombic high-pressure phase is Pbcm; if we assume that the o-ZrO_2 phase discussed in this paper is isostructural with this high-pressure phase, then the point group of this structure is mmm. Moreover the TEM observations indicate that the transformation is displacive but not martensitic (quasi-martensitic in the terminology of Cohen *et al.* [46]), and involves only small displacements of the oxygen atoms. It is therefore possible to apply group-theoretical considerations to predict the number of rotational and translational variants.

For the sake of brevity, only the essential results will be given; the interested reader is referred to the original paper of Van Tendeloo and Amelinckx [47] for further details of the theoretical analysis.

The point group G of the tetragonal prototype phase is 4/mmm (space group $P4_2/nmc$) and contains the 16 symmetry elements represented in Fig. 9a. The point group H of the orthorhombic phase is, as mentioned earlier, mmm, a subgroup of 4/mmm, and contains 8 symmetry elements (Fig. 9b). From a group-theoretical point of view the group G can be decomposed in terms of co-sets of the subgroup H in the following manner:

$$G = EH + gH$$

where E is the identity symmetry operation and g is an element of G but not an element of H. The sets EH and gH mean that all elements of H $(h_1, h_2, \ldots, h_8)$ are multiplied by E and g, respectively. In our case the set-theoretic sum is given by

$$G = EH + C_4H$$

where C_4 is the four fold axis of the original tetragonal structure. The two sets EH and C_4H have no elements in common.

From this simple analysis it can be concluded that the t → o transformation gives rise to two orthorhombic rotational variants. The two orthorhombic variants are related by a rotation of 90° about the c axis of the original tetragonal structure, giving rise to permutation boundaries between the variants (the a and b axes of the orthorhombic phase are permuted).

The number of translational variants for a given rotational variant is simply given by the ratio α of the volume of the primitive unit cells of the product and parent phase. However, for the tetragonal structure it is more convenient to use a doubly primitive unit cell; therefore we multiply α by 2, which is the multiplicity of the non-primitive tetragonal unit cell, and since we can neglect the small fractional volume change involved in the transformation (see Table I), we conclude that there are two translational variants associated with each rotational variant, and they are separated by an antiphase domain vector $\frac{1}{2}[1\,1\,0]_o$ which is consistent with experiment [34].

4. Discussion and conclusion

It appears that the occurrence of the t → o transformation is ubiquitous in all ZrO_2-based materials during TEM study. The diffraction information is consistent with the proposed space groups Pbcm and Pbca for o- and o′-ZrO_2, respectively, although we have not attempted further refinements of the crystallography (using convergent-beam techniques, for example). Comparing the several materials studied, several similarities and differences can be noted.

Firstly, the transformation is most easily induced in Mg-PSZ. One possible explanation is the small increase in volume (see Table I) associated with the transformation in Mg-PSZ. Secondly, linear defects are often present in o-ZrO_2 in Mg-PSZ, Ca-PSZ and ZTA, giving rise to streaks in some SAD patterns, while in the case of Y-PSZ and a (Mg, Y)-PSZ (not discussed in this paper), and possibly in Mg-PSZ as well, APBs can be present (these APBs are not observed in the other systems). More work needs to be done to understand these different transformation microstructures in the several systems.

Finally, by comparing the calculated lattice parameters of o-ZrO_2 to the lattice parameters of the tetragonal and monoclinic polymorphs, the unit cell volume of the orthorhombic phase is always between that of the tetragonal and monoclinic cells. This is expected, as the reaction product of the t → o transformation can be thought of as an intermediate stage, facilitated by the thin-foil conditions, in the t → m transformation. Given that the density of o-ZrO_2 is higher than that of m-ZrO_2 but lower than for t-ZrO_2, it is also clear that while o-ZrO_2 is a high-pressure phase relative to m-ZrO_2, and will only form under hydrostatic confining pressure, it is a low-pressure phase relative to t-ZrO_2, and so forms readily as an artefact in thin foils.

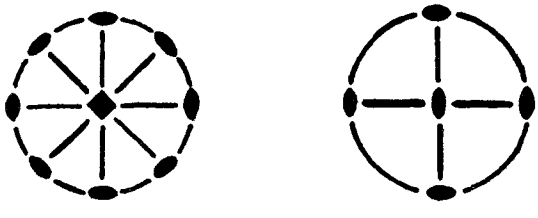

Figure 9 Stereographic projections showing the symmetry elements of (a) 4/mmm point group, (b) mmm point group.

Acknowledgements

The research was supported by the NSF under Grant No. DMR82-14128 (Mg-PSZ, Ca-PSZ, (Mg, Y)-PSZ) and DOE under Grant No. DEFG9284ER 45110 (Y-PSZ, ZTA). We thank S. Kraus-Lanteri for Fig. 8.

References

1. J. D. McCULLOUGH and K. N. TRUEBLOOD, *Acta Crystallogr.* **12** (1959) 507.

2. L. N. KOMISSAROVA, Yu. P. SIMANOV and Z. A. VLADIMIROVA, *Russ. J. Inorg. Chem.* **5** (1960) 687.
3. G. TEUFER, *Acta Crystallogr.* **15** (1962) 1187.
4. D. K. SMITH and H. W. NEWKIRK, *ibid.* **18** (1965) 983.
5. G. KATZ, *J. Amer. Ceram. Soc.* **54** (10) (1971) 531.
6. P. ALDEBERT and J. P. TRAVERSE, *ibid.* **68** (1) (1985) 34.
7. R. E. HANN, P. R. SVITCH and J. L. PENTECOST, *ibid.* **68** (10) (1985) C285.
8. H. G. SCOTT, *J. Mater. Sci.* **10** (1975) 1527.
9. R. A. MILLER, J. L. SMIALEK and R. G. GARLICK, in "Advances in Ceramics", Vol. 3, edited by A. H. Heuer and L. W. Hobbs (American Ceramic Society, Columbus, Ohio, 1981) p. 241.
10. D. MICHEL, L. MAZEROLLES and M. PEREZ y JORBA, *J. Mater. Sci.* **18** (1983) 2618.
11. V. LANTERI, T. E. MITCHELL and A. H. HEUER, in "Advances in Ceramics", Vol. 12, edited by N. Claussen, M. Ruhle and A. H. Heuer (American Ceramic Society, Columbus, Ohio, 1984) p. 118.
12. R. CHAIM, M. RUHLE and A. H. HEUER, *J. Amer. Ceram. Soc.* **68** (8) (1985) 427.
13. A. H. HEUER, R. CHAIM and V. LANTERI, *Acta Metall.* **3** (1987) 661.
14. A. H. HEUER and L. W. HOBBS (eds), "Advances in Ceramics", Vol. 3 (American Ceramic Society, Columbus, Ohio, 1981).
15. N. CLAUSSEN, M. RUHLE and A. H. HEUER (eds), "Advances in Ceramics", Vol. 12 (American Ceramic Society, Columbus, Ohio, 1984).
16. H. HASEWAGA, *J. Mater. Sci. Lett.* **2** (1983) 91.
17. H. HASEWAGA, T. HIOKI and O. KAMIGAITO, *ibid.* **4** (1985) 1092.
18. N. A. BENDELIANI, S. V. POPOVA and L. P. VERSCHAGIN, *Geokhimiya* **6** (1967) 677.
19. G. BOCQUILLON and C. SUSSE, *Rev. Int. Hautes Temp. Refract.* **6** (1969) 263.
20. L. G. LIU, *J. Phys. Chem. Solids* **41** (1980) 331.
21. S. BLOCK, J. A. H. Da JORNADA and G. J. PIERMARINI, *J. Amer. Ceram. Soc.* **68** (9) (1985) 497.
22. R. SUYAMA, T. ASHIDA and S. KUME, *ibid.* **68** (12) (1985) C314.
23. Y. KUDOH, H. TAKEDA and H. ARASHI, *Phys. Chem. Miner.* **13** (1986) 233.
24. L. LENZ and A. H. HEUER, *J. Amer. Ceram. Soc.* **65** (11) (1982) C192.
25. L. H. SCHOENLEIN and A. H. HEUER, in "Fracture Mechanics of Ceramics", Vol. 6, edited by R. C. Bradt, A. G. Evans, D. P. H. Hasselman and F. F. Lange (Plenum, New York, 1983) pp. 309–323.
26. A. H. HEUER and L. H. SCHOENLEIN, *J. Mater. Sci.* **20** (1985) 3421.
27. A. H. HEUER, L. H. SCHOENLEIN and S. C. FARMER, "Science of Ceramics 12" (Ceramurgica, Faenza, Italy, 1983) pp. 257–266.
28. L. H. SCHOENLEIN, PhD thesis, Case Western Reserve University (1982).
29. B. C. MUDDLE, in "Advanced Structural Ceramics", edited by P. F. Becher, M. V. Swain and S. Somiya, Material Research Symposium Proceedings Vol. **78** (1987) 3.
30. T. A. BIELICKI, H. DAHMEN, G. THOMAS and K. H. WESTMACOTT, in Proceedings of "ZrO_2 '86", in "Advances in Ceramics", Vol. 24, edited by S. Somiya, N. Yamamoto and H. Yanagida (American Ceramic Society, Columbus, Ohio, 1988) in press.
31. Y. H. CHIAO and I-WEI CHEN, in "Grain Boundary Structure and Related Phenomena", Proceedings of JIMIS No. 4, *Trans. Jap. Inst. Metals* **27** (Suppl.) (1986) 197–203.
32. R. M. DICKERSON, M. SWAIN and A. H. HEUER, *J. Amer. Ceram. Soc.* **70** (4) (1987) 214.
33. A. H. HEUER, R. CHAIM, and V. LANTERI in Proceedings of "ZrO_2 '86", in "Advances in Ceramics", Vol. 24, edited by S. Somiya, N. Yamamoto and H. Yanagida (American Ceramic Society, Columbus, Ohio, 1988) in press.
34. H. BESTGEN, R. CHAIM and A. H. HEUER, *J. Amer. Ceram. Soc.* in press.
35. R.-R. LEE and A. H. HEUER, *ibid.* **71** (8) (1988) 694–700.
36. D. B. MARSHALL, M. JAMES and R. J. PASTER, *ibid.* (in press).
37. H. ARASHI, in Proceedings of "ZrO_2 '86", in "Advances in Ceramics", Vol. 24, edited by S. Somiya, N. Yamamoto and H. Yanagida (American Ceramic Society, Columbus, Ohio, 1988) in press.
38. V. LANTERI, T. E. MITCHELL and A. H. HEUER, *J. Amer. Ceram. Soc.* **69** (7) (1986) 564.
39. N. ISHIZAWA, A. SAIKI, J. JOGI, N. MIZUTANI and M. KATO, *ibid.* **69** (2) (1986) C18.
40. M. SHIBATA-YANAGISAWA, M. KATO, H. SETO, N. ISHIZAWA, N. MIZUTANI and M. KATO, *ibid.* **70** (7) (1987) 505.
41. A. H. HEUER, V. LANTERI and R. CHAIM, *Ultramicrosc.* **22** (1987) 27.
42. J. M. MARDER, T. E. MITCHELL and A. H. HEUER, *Acta. Metall.* **31** (1983) 387.
43. R.-R. LEE and A. H. HEUER, *J. Amer. Ceram. Soc.* **70** (4) (1987) 208.
44. B. W. KIBBEL and A. H. HEUER, to be published.
45. M. A. O'KEEFE and P. R. BUSECK, *Trans. Amer. Crystallogr. Assoc.* **15** (1) (1979) 27.
46. M. COHEN, G. B. OLSEN and P. C. CLAPP, in Proceedings of International Conference on Martensitic Transformations, Cambridge, Massachusetts, 1979, p. 1.
47. G. VAN TENDELOO and S. AMELINCKX, *Acta Crystallogr.* **A30** (1974) 431.

Received 15 September 1987
and accepted 26 January 1988